Journal of
Materials Chemistry

Dynamic Article Links View Online

Cite this: *J. Mater. Chem.*, 2011, **21**, 5230

www.rsc.org/materials

COMMUNICATION

Simple route to ridge optical waveguide fabricated *via* controlled evaporative self-assembly

Soon Woo Kwon,[ad] Myunghwan Byun,[b] Dae Ho Yoon,[a] Jun-Hee Park,[c] Woo-Kyung Kim,[d] Zhiqun Lin*[b] and Woo Seok Yang*[d]

Received 24th December 2010, Accepted 31st January 2011
DOI: 10.1039/c0jm04514d

Downloaded on 26 March 2011
Published on 07 March 2011 on http://pubs.rsc.org | doi:10.1039/C0JM04514D

A simple route to intriguing patterns for optical waveguides was demonstrated by controlled evaporative self-assembly (CESA) of confined microfluid. Silica ridge waveguides were fabricated by applying wet and dry etching based on stripe patterns formed by CESA. The optical mode of the resulting waveguides was confirmed by exposing them to the 1064 nm transmission light.

Because of increased interest in the development of integrated hybrid optoelectronic devices for use in photonic sensors and communication services, new methods for device fabrication by utilizing simple, fast and inexpensive process are highly desirable.[1–3] In this regard, drying-mediated self-assembly of non-volatile solutes (polymers, nanocrystals, nanoparticles, nanorods and DNA) through irreversible solvent evaporation has received considerable attention for its ease of producing complex, large-scale structures in one-step for potential applications in micro-electronics, optoelectronics and biotechnology.[4–29] Recently, it has been demonstrated that highly organized structures with controlled size and shapes over large areas can be achieved by precisely regulating the solvent evaporation process in a restricted geometry composed of a curved surface situated on a flat substrate (curve-on-flat geometry).[13–29] The repetitive "stick–slip" motion (*i.e.*, pinning–depinning) of a three-phase contact line of the evaporating drop was effectively controlled in such a restricted geometry, forming well-ordered coffee ring-like deposits.[13,14] Notably, by rationally designing the upper curved surface of the restricted geometry to accommodate different shapes, more intriguing and complex patterns can be readily created.[15] Such regularly organized, complex structures can be considered as device-oriented structures and may potentially be integrated into microelectronic, optical, optoelectronic, and sensing devices.[15]

[a]*School of Advanced Materials Science and Engineering, Sungkyunkwan University, Suwon, 440-746, Republic of Korea*
[b]*Department of Materials Science and Engineering, Iowa State University, Ames, IA, 50011, USA. E-mail: zqlin@iastate.edu; Fax: +515 294 7202; Tel: +515 294 9967*
[c]*School of Electrical and Computer Engineering, University of Seoul, Seoul, 130-743, Republic of Korea*
[d]*Electronic Materials and Device Research Center, Korea Electronics Technology Institute, Seongnam, 463-816, Republic of Korea. E-mail: wsyang@keti.re.kr; Fax: +82 31 789 7249; Tel: +82 31 789 7256*

The patterns formed by the aforementioned controlled evaporative self-assembly (CESA) have been utilized as templates for pattern transferring to underlying substrates to produce a variety of metal and metal oxide microstructures with unprecedented regularity or direct the deposition of carbon nanotubes with the controlled density in a gradient concentric fashion.[16,21,22] Clearly, the non-lithographic technique based on CESA in a restricted geometry may possibly yield versatile templates for the fabrication of hybrid optoelectronic devices including optical waveguides that only require stripe patterns. To date, most rib-type optical waveguides have been fabricated using expensive photolithography in which multi-step processes are involved.[30–33]

Herein, we report on a new inexpensive approach to fabricate rib-type silica optical waveguides by sequentially performing plasma-enhanced chemical vapor deposition (PECVD) of a silica layer, e-beam evaporation of a Ni–Cr thin film, CESA of polymer solution in a cylinder-on-flat geometry, selective etching of uncovered Ni–Cr using wet chemical etchant, elimination of polymer patterns on the top of polymer-covered Ni–Cr stripes, partial etching of a silica layer using neutral loop discharge (NLD) plasma etcher, and removal of the Ni–Cr stripe protective layer. The resulting rib-type silica wave-guides possess a length of 5 mm and a thickness of 550 nm in a gradient fashion.

A newly designed cylinder-on-flat geometry in which an upper cylindrical lens was situated on a lower stationary flat substrate with a drop of PMMA–toluene solution loaded and trapped is shown in Fig. 1a and b (3D view in Fig. 1a and 2D cross-sectional view in Fig. 1b), thereby forming a capillary-held solution (see Experimental section).[13,20] The flat substrate was composed of a Ni–Cr thin film on a silica layer supported on a fused silica glass substrate (*i.e.*, the Ni–Cr/silica layer/fused silica glass substrate, see Experimental section). To form the core layer of waveguides, a 3 μm silica layer with refractive index of 1.476 was deposited on the fused silica glass by PECVD. As a passivation layer for the dry etching process, a 250 nm Ni–Cr film was deposited on the silica layer using e-beam evaporator (Fig. 1a and b; see Experimental section).

The abovementioned apparatus was encapsulated in a constant humidity chamber so that the solvent evaporation rate was controlled and the temperature gradient was eliminated.[13] As toluene evaporated from the capillary edge, the initial contact angle of the meniscus gradually decreased and the non-volatile solute PMMA transported to the edge to pin the contact line due to the outward flow of PMMA

 This journal is © The Royal Society of Chemistry 2011

View Online

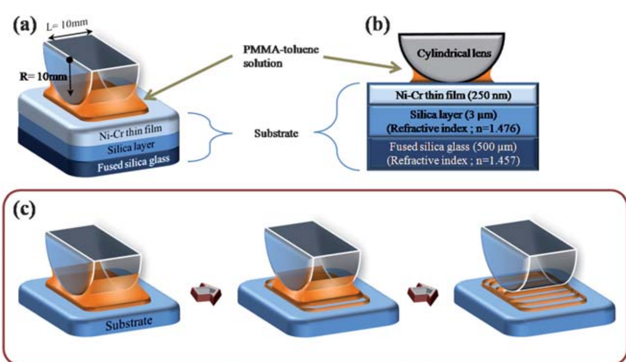

Fig. 1 (a–b) Schematic illustration of the cylinder-on-flat geometry in which a PMMA–toluene solution was trapped (a: 3D view, and b: cross-sectional view). (c) Schematic representation of the formation of global gradient PMMA rectangles. A drop of PMMA–toluene solution was loaded in a restricted geometry consisting of a cylindrical lens on a flat substrate (*i.e.*, cylinder-on-flat geometry), forming a capillary-held solution. As the contact line of trapped solution retracted toward the cylinder/flat substrate contact center by successive controlled "stick–slip" motions, gradient rectangles of PMMA over large areas were produced, which served as the template to fabricate silica ridge waveguides.

driven by the solvent evaporation. When the contact angle was below the critical value, the depinning force (*i.e.*, capillary force) became larger than the pinning force (*i.e.*, friction force); this led the contact line to jerk to next position toward the cylinder/flat substrate contact center, leaving behind a rectangular-shaped deposit of PMMA (the second panel in Fig. 1c). The contact line was arrested again at this new position as toluene evaporated, forming the second PMMA rectangle inward that was adjacent to the first deposit. This "pinning–depinning" process (*i.e.*, "stick–slip" motion) continued until the complete evaporation of solvent, forming concentric rectangles as illustrated in the last panel of Fig. 1c. It is worth noting that the use of cylinder as the upper surface provided a unique environment to guide the deposition of PMMA that conformed to the shape of cylinder, thereby leading to highly ordered concentric PMMA rectangles.

Fig. 2 shows the optical micrographs of the PMMA patterns over large areas created by controlled evaporative self-assembly (CESA). Locally, they appeared as parallel stripes. The patterns were annealed

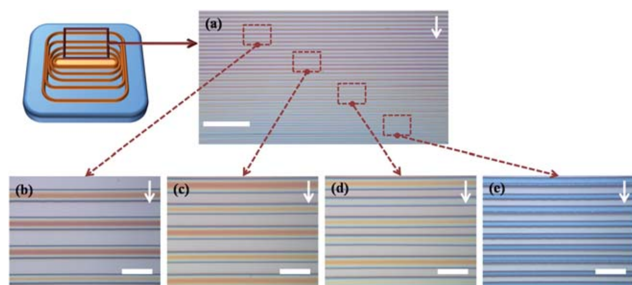

Fig. 2 Optical micrographs of PMMA patterns formed by CESA of the PMMA–toluene solution in the cylinder-on-flat geometry. (a) Locally, the patterns appeared as parallel stripes. Scale bar = 500 μm. (b–e) The width and height of stripes as well as the characteristic distance between adjacent stripes gradually decreased as PMMA progressively deposited toward the cylinder/flat substrate contact center during the course of solvent evaporation. The arrows on the upper right of each image mark the direction of the movement of the solution front. Scale bar = 50 μm.

at 180 °C for 1 h to prevent possible delamination from the Ni–Cr/silica layer/fused silica glass substrate during chemical etching process. The number of PMMA stripes in a representative optical micrograph was approximately 50 (Fig. 2a). They exhibited gradient in width, w, and height, h, as the deposition of PMMA stripes moved toward the cylinder/flat substrate contact center,[13,15] changing from $w = 23.5 \pm 3.6$ μm and $h = 212.5 \pm 12.5$ nm (Fig. 2b), to $w = 23.6 \pm 3.8$ μm and $h = 225 \pm 5$ nm (Fig. 2c), to $w = 20.4 \pm 2.6$ μm and $h = 175 \pm 25$ nm (Fig. 2d), and to $w = 13.4 \pm 3.9$ μm and $h = 100 \pm 10$ nm (Fig. 2e). The same trend for the characteristic distance between adjacent rectangles, λ was observed, progressively decreasing from $\lambda = 48.1 \pm 1.7$ μm (Fig. 2b), to 41.4 ± 0.7 μm (Fig. 2c), to 34.3 ± 1 μm (Fig. 2d), and to 23.8 ± 1.9 μm (Fig. 2e) as the solution front approached the cylinder/flat substrate contact center.

Subsequently, the PMMA patterns were utilized to fabricate rib-type optical waveguides by successive etching processes, both wet and dry etching, as schematically illustrated in Fig. 3a–e. The cross-sectional height profile and 3D AFM height images corresponding to the steps in Fig. 3a–e are shown in Fig. 3g–k. The O_2 plasma asher was employed to remove any possible trace amount of PMMA deposited between neighboring PMMA stripes during the depinning process (Fig. 3a and g), which would otherwise lead to the formation

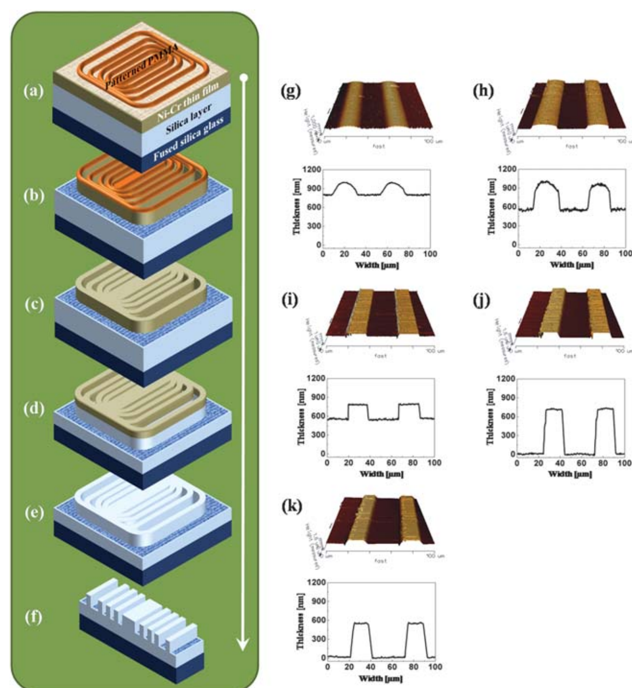

Fig. 3 (a–f) Stepwise representation of the waveguide fabrication using the PMMA template prepared by controlled evaporative self-assembly of PMMA–toluene solution (Fig. 1). The corresponding 3D AFM height images and 2D profiles are shown in (g–k). (a and g) PMMA patterns that served as a template. (b and h) Selective removal of the Ni–Cr film that was uncovered by the PMMA template using appropriate wet etching solution. (c and i) Elimination of PMMA patterns with acetone, thereby exposing the Ni–Cr patterns underneath. (d and j) Dry-etching of the top silica core layer between Ni–Cr patterns by the NLD plasma etcher, yielding a 550 nm depth in the silica core layer. (e and k) After wet-etching of the Ni–Cr passivation layer, the silica ridge waveguide with 550 nm height and 20 μm width supported on the fused silica layer was created. (f) The waveguides with parallel stripes were diced into 5 mm in length and polished for optical measurement.

Downloaded on 26 March 2011
Published on 07 March 2011 on http://pubs.rsc.org | doi:10.1039/C0JM04514D

View Online

of a rough surface and ultimately influence the signal attenuation and cause the optical loss of the resulting optical waveguides. The PMMA stripes were served as a template; a 250 nm thick Ni–Cr film that was uncovered by the PMMA template was then selectively removed by an appropriate wet etching solution (Fig. 3b and h; see Experimental section), followed by eliminating the PMMA template with acetone, thus leaving behind isolated Ni–Cr stripes (Fig. 3c and i).

The silica ridge waveguides supported on the fused silica glass substrate (*i.e.*, a high refractive index layer on a lower index foundation) were obtained after dry-etching of the top core silica layer between the Ni–Cr stripes using the NLD plasma etcher (Fig. 3d and j) and subsequently wet-etching of the Ni–Cr passivation layer (Fig. 3e and k). The thickness and width of waveguides were 550 nm and 20 μm, respectively as shown in Fig. 3k. For such rib-type waveguides, the high-index core layer was not fully etched (*i.e.*, 550 nm thick as compared to a 3 μm initially deposited silica layer) as the difference between the effective refractive indexes of partially etched slab and rib could be sufficient to confine light within the rib section.[34,35] Finally, the waveguides with parallel stripes were diced into 5 mm in length for the polishing process of cross-sections and subsequent optical measurements (Fig. 3f). It is noteworthy that optical characteristic of waveguides is typically affected by their sidewall roughness. Because of the non-uniform sidewall roughness of fabricated waveguides, an incident light did not penetrate the waveguides with narrow width and thick depth and led to the scattering during the propagation of light in waveguides. For the waveguides of 10 μm wide and 2.5 μm thick made in the present study, optical characteristic was not confirmed and optical mode was not obtained. Based on this result, the width and thickness of waveguides were judiciously fabricated to reduce the sidewall effect. Consequently, the waveguide with 20 μm width (Fig. 3g) and 550 nm thick was produced and analyzed for optical measurement.

Fig. 4a depicts the optical measurement of waveguides. The laser diode with a wavelength of 1064 nm, single mode fiber, and fiber block were used for a single mode excitation of incident light. The near field patterns of a waveguide mode were collected by a charge coupled device (CCD) camera. The SEM image of fabricated ridge waveguide is shown in Fig. 4b (top view); the width of measured silica waveguide was about 20 μm. The shape of optical mode taken by the CCD camera is displayed in Fig. 4c; the 1064 nm transmission light was guided through the optical waveguide and its optical mode was found to be multi-mode.[1,36]

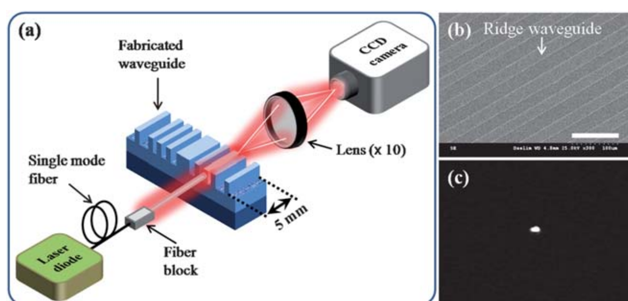

Fig. 4 (a) Schematic illustration of the optical measurement for the resulting waveguides. (b) SEM image of the fabricated ridge waveguide (top view). Scale bar = 100 μm. The height of these waveguides is identical to those shown in Fig. 3k. (c) The shape of optical mode taken by a charge coupled device (CCD) camera using the transmission light at the 1064 nm wavelength.

Experimental section

Poly (methyl methacrylate) (PMMA; number-average molecular weight, M_n = 133 kg mol^{-1}; polydispersity index, PDI = 1.64) was selected as the non-volatile solute to prepare PMMA stripes that served as a template to yield the Ni–Cr stripes. The PMMA–toluene solution at the concentration of 0.8 mg mL^{-1} was prepared by dissolving PMMA in toluene and purified with 0.2 μm hydrophobic membrane filter.

A fused silica glass substrate with refractive index of 1.457 at the wavelength of 633 nm was used as a lower clad layer for waveguides. To fabricate the silica ridge waveguides, a 3 μm silica layer and a 250 nm Ni–Cr (80 : 20 wt%) thin film were sequentially deposited on the fused silica glass substrate by using plasma-enhanced chemical vapor deposition (PECVD) and e-beam evaporator, respectively (Fig. 1b). PECVD was performed at a radio-frequency (RF) of 13.56 MHz and a substrate temperature of 300 °C. The SiH_4, N_2 and N_2O flow rates were fixed at 29.2 sccm, 1500 sccm and 700 sccm, respectively. The RF power and working pressure were 100 W and 1700 mTorr, respectively.[37] Generally, PECVD yields better film uniformity and rapid deposition rate than the low-pressure chemical vapor deposition (LPCVD) or sputtering.

To produce polymer patterns for the fabrication of optical waveguides, a cylindrical lens with 10 mm in length and 10 mm in radius was utilized, and placed above the flat Ni–Cr–silica-layer-coated fused silica glass substrate (*i.e.*, the Ni–Cr/silica layer/fused silica glass substrate) in a constant humidity chamber. A drop of 30 μL PMMA–toluene solution was loaded and trapped between the substrate and the cylindrical lens due to the capillary force. Finally, the cylindrical lens was brought into firm contact with the substrate, forming a capillary-held solution with the highest solvent evaporation rate at the edge of the capillary (cylinder-on-flat geometry; Fig. 1a).[13] As toluene evaporated, the concentric PMMA stripes were formed on the Ni–Cr thin film surface as a result of repetitive "stick–slip" motion of the three-phase contact line of the evaporating PMMA solution in the cylinder-on-flat geometry (Fig. 1c). The evaporation was typically completed in less than 30 minutes. After that, the substrate and cylindrical lens were separated. The structures formed on the flat Ni–Cr-coated substrate were examined by optical microscope and atomic force microscopy (AFM).

The O_2 plasma asher was applied to remove possible trace amount of PMMA between the PMMA stripes. Subsequently, the Ni–Cr stripes were achieved by selective removal of the Ni–Cr thin film unprotected by the PMMA stripes using Cr etchant (CR-7SK, CYANTEK Co.) (Fig. 3b), followed by elimination of PMMA by acetone (Fig. 3c). The rib-type silica waveguides with a uniform thickness of 550 nm were thus produced by the high density NLD plasma etcher after removing the Ni–Cr stripes (Fig. 3d). The resulting waveguides with parallel stripes were diced into 5 mm in length and polished for subsequent optical measurements (Fig. 3e and f). The optical mode of waveguides was confirmed using the 1064 nm transmission light.

Conclusions

In summary, we present a new preparative method to rationally design and fabricate silica ridge optical waveguides in a simple, cost-effective manner, dispensing with the need for the conventional lithography. The method is based on the controlled evaporative

Published on 07 March 2011 on http://pubs.rsc.org | doi:10.1039/C0JM04514D
Downloaded on 26 March 2011

This journal is © The Royal Society of Chemistry 2011

View Online

self-assembly (CESA) of polymer solution constrained in a cylinder-on-flat geometry with subsequent wet and dry etching of the sacrificial Ni–Cr film, the deposited polymer template, and the silica layer. The resulting ridge waveguide was measured using 1064 nm transmission light, exhibiting a multi-mode optical characteristic. Notably, the multi-mode waveguides have widely been exploited as optical sensors such as interferometer and refractometer.[38,39] The waveguides fabricated by the present approach may find potential applications as optical sensors. This study is currently undergoing.

Acknowledgements

We gratefully acknowledge financial support from the Korea Electronics Technology Institute and the National Science Foundation (NSF CAREER Award (CBET-0844084)).

References and notes

1 E. Kim, G. M. Whitesides, L. K. Lee, S. P. Smith and M. Prentiss, *Adv. Mater.*, 1996, **8**, 139.
2 H. Ma, A. K.-Y. Jen and L. R. Dalton, *Adv. Mater.*, 2002, **14**, 1339.
3 G.-S. Son, W.-K. Kim, W.-S. Yang, H.-M. Lee, H.-Y. Lee, S.-D. Lee, W.-J. Jeong, S.-W. Kwon, Y.-N. Kim and S.-S. Lee, *Opt. Lett.*, 2009, **34**, 2045.
4 T. P. Bigioni, X. M. Lin, T. T. Nguyen, E. I. Corwin, T. A. Witten and H. M. Jaeger, *Nat. Mater.*, 2006, **5**, 265.
5 M. Gleiche, L. F. Chi and H. Fuchs, *Nature*, 2000, **403**, 173.
6 Z. Q. Lin and S. Granick, *J. Am. Chem. Soc.*, 2005, **127**, 2816.
7 B. G. Prevo and O. D. Velev, *Langmuir*, 2004, **20**, 2099.
8 H. Hu and R. G. Larson, *Langmuir*, 2005, **21**, 3963.
9 J. Huang, F. Kim, A. R. Tao, S. Connor and P. D. Yang, *Nat. Mater.*, 2005, **4**, 896.
10 K. L. Genson, J. Hoffman, J. Teng, E. R. Zubarev, D. Vaknin and V. V. Tsukruk, *Langmuir*, 2004, **20**, 9044.
11 K. L. Genson, J. Holzmueller, C. Jiang, J. Xu, J. D. Gibson, E. R. Zubarev and V. V. Tsukruk, *Langmuir*, 2006, **22**, 7011.
12 B. P. Khanal and E. R. Zubarev, *Angew. Chem., Int. Ed.*, 2007, **46**, 2195.
13 J. Xu, J. Xia, S. W. Hong, Z. Q. Lin, F. Qiu and Y. L. Yang, *Phys. Rev. Lett.*, 2006, **96**, 066104.
14 J. Xu, J. Xia and Z. Q. Lin, *Angew. Chem., Int. Ed.*, 2007, **46**, 1860.
15 S. W. Hong, M. Byun and Z. Q. Lin, *Angew. Chem., Int. Ed.*, 2009, **48**, 512.
16 S. W. Hong, S. Giri, V. S. Y. Lin and Z. Q. Lin, *Chem. Mater.*, 2006, **18**, 5164.
17 S. W. Hong, J. Wang and Z. Q. Lin, *Angew. Chem., Int. Ed.*, 2009, **48**, 8356.
18 S. W. Hong, J. Xia, M. Byun, Q. Zou and Z. Q. Lin, *Macromolecules*, 2007, **40**, 2831.
19 S. W. Hong, J. Xia and Z. Q. Lin, *Adv. Mater.*, 2007, **19**, 1413.
20 S. W. Hong, J. Xu, J. Xia, Z. Q. Lin, F. Qiu and Y. L. Yang, *Chem. Mater.*, 2005, **17**, 6223.
21 S. W. Hong, W. Jeong, H. Ko, M. R. Kessler, V. Tsukruk and Z. Q. Lin, *Adv. Funct. Mater.*, 2008, **18**, 2114.
22 S. W. Hong, J. Xu and Z. Q. Lin, *Nano Lett.*, 2006, **6**, 2949.
23 M. Byun, N. B. Bowden and Z. Q. Lin, *Nano Lett.*, 2010, **10**, 3111.
24 M. Byun, W. Han, F. Qiu, N. B. Bowden and Z. Q. Lin, *Small*, 2010, **6**, 2250.
25 M. Byun, S. W. Hong, F. Qiu, Q. Zou and Z. Lin, *Macromolecules*, 2008, **41**, 9312.
26 M. Byun, S. W. Hong, L. Zhu and Z. Q. Lin, *Langmuir*, 2008, **24**, 3525.
27 M. Byun, R. L. Laskowski, M. He, F. Qiu, M. Jeffries-EL and Z. Q. Lin, *Soft Matter*, 2009, **5**, 1583.
28 M. Byun, J. Wang and Z. Lin, *J. Phys.: Condens. Matter*, 2009, **21**, 264014.
29 M. Byun, J. Wang and Z. Lin, *Acta Phys.-Chim. Sin*, 2009, **25**, 1249.
30 F. Prieto, A. Llobera, D. Jimenez, C. Domenguez, A. Calle and L. M. Lechuga, *J. Lightwave Technol.*, 2000, **18**, 966.
31 C. Grivas, D. P. Shepherd, T. C. May-Smith and R. W. Eason, *Opt. Express*, 2005, **13**, 210.
32 Y. Ruan, W. Li, R. Jarvis, N. Madsen, A. Rode and B. Luther-Davies, *Opt. Express*, 2004, **12**, 5140.
33 B. Cakmak, *Opt. Express*, 2002, **10**, 530.
34 K. Worhoff, P. V. Lambeck and A. Driessen, *J. Lightwave Technol.*, 1999, **17**, 1401.
35 N. Dagli and C. G. Fonstad, *IEEE J. Quantum Electron.*, 1985, **21**, 315.
36 L. B. Soldano and E. C. M. Pennings, *J. Lightwave Technol.*, 1995, **13**, 615.
37 Q. Wang and G. Farrell, *Opt. Lett.*, 2006, **31**, 317.
38 J. J. Ju, S. K. Park, S. Park and J. Kim, *Appl. Phys. Lett.*, 2006, **88**, 241106.
39 Z. M. Qi, N. Matsuda, J. H. Santos, A. Takatsu and K. Kato, *Opt. Lett.*, 2002, **27**, 689.

Published on 07 March 2011 on http://pubs.rsc.org | doi:10.1039/C0JM04514D
Downloaded on 26 March 2011